Nano Res (2009) 2: 130–134
DOI 10.1007/s12274-009-9010-2
Research Article

Bi_2S_3 Nanotubes: Facile Synthesis and Growth Mechanism

Dingsheng Wang, Chenhui Hao, Wen Zheng, Xiaoling Ma, Deren Chu, Qing Peng, and Yadong Li (✉)

Department of Chemistry, Tsinghua University, Beijing 100084, China

Received: 22 October 2008 / Revised: 4 December 2008 / Accepted: 4 December 2008

ABSTRACT

Synthesis of tubular nanomaterials has become a prolific area of investigation due to their wide range of applications. A facile solution-based method has been designed to fabricate uniform Bi_2S_3 nanotubes with average size of 20 nm × 160 nm using only bismuth nitrate ($Bi(NO_3)_3{\cdot}5H_2O$) and sulfur powder (S) as the reactants and octadecylamine (ODA) as the solvent. Powder X-ray diffraction (XRD), transmission electron microscopy (TEM), high-resolution TEM (HRTEM), and energy dispersive spectroscopy (EDX) experiments were employed to characterize the resulting Bi_2S_3 nanotubes and the classic rolling mechanism was applied to explain their formation process.

KEYWORDS

Bi_2S_3, nanotubes, solution-based synthesis, rolling mechanism

Introduction

Since the discovery of carbon nanotubes in 1991, tubular nanostructures of materials have attracted enormous attention due largely to their distinctive physical and chemical properties and potential applications in nanodevices, nanobiology, and nanocatalysis [1–8]. For example, because of their unique tubular topology, nanotubes might be promising candidates for electrode materials in Li-ion batteries which are the most advanced power sources for modern portable electronic devices [9–13]. Actually, studies by Shimoda et al. have indeed demonstrated the increased charge capacity of single-walled carbon nanotubes (SWNTs) [11]. A wide variety of dichalcogenide nanotubes such as MoS_2 and WS_2 have also been considered for cathode materials in Li-ion batteries [12, 13].

Bismuth sulfide (Bi_2S_3), a very important photoconductive, direct band gap (E_g = 1.3 eV) semiconductor, has numerous significant applications including in photovoltaic converters, photodiode arrays, and thermoelectric cooling technologies based on the Peltier effect [14, 15]. Recently, the excellent electrochemical hydrogen storage properties of Bi_2S_3 flower-like patterns with well-aligned nanorods and disc-like Bi_2S_3 nanorod networks have been investigated by the Xie and Qi groups, respectively [16, 17]. However, Bi_2S_3 nanotubes are still difficult to exploit in industrial applications. The reason is probably that there exist great challenges to obtain high quality Bi_2S_3 nanotubes using a simple, inexpensive, and efficient approach [18–20].

Although various methods have been developed for the fabrication of 1-D Bi_2S_3 nanostructures including nanorods, nanowires, and nanoribbons,

Address correspondence to ydli@mail.tsinghua.edu.cn

investigation of nanotube synthesis is quite rare [21, 22]. Only in 2002, Bi_2S_3 nanotubes were obtained for the first time by Ye's group through the conventional evaporation method using nanometer-sized Bi_2S_3 particles as starting materials [18]. The chemical vapor deposition approach requires high temperature and the low throughput of final products also limits its applications. In 2005, Srivastava et al. successfully synthesized Bi_2S_3 nanotubes using Triton-X 100 as the template in the second report of the growth of Bi_2S_3 nanotubes [19]. Very recently, Shen and co-workers prepared single crystalline Bi_2S_3 nanotubes by pyrolyzing a single-source precursor $Bi(S_2CNEt_2)_3$ at 530 °C [20]. In the present work, a facile, low temperature, and template-free method to synthesize high-quality Bi_2S_3 nanotubes is presented. Using only $Bi(NO_3)_3{\cdot}5H_2O$ and S as the reactants and octadecylamine (ODA) as the solvent, we could obtain Bi_2S_3 nanotubes with average size of 20 nm× 160 nm. Their structural characterization, the growth process, formation mechanism are discussed.

1. Experimental

Materials. All the reagents used in this work, including $Bi(NO_3)_3{\cdot}5H_2O$, S, ODA, ethanol, and cyclohexane, were of analytical grade from the Beijing Chemical Factory. They were used without further purification.

Synthesis. Briefly, Bi_2S_3 nanotubes with average size of 20 nm×160 nm were made by adding $Bi(NO_3)_3{\cdot}5H_2O$ (0.1 g) and S (0.05 g) to solvent ODA (10 mL) at 100 °C. The mixture was magnetically stirred for 4 h in air and subsequently heated to 200 °C and stirred for another 10 min. The system was then allowed to cool to 80 °C (the melting point of ODA) and the final products were collected at the bottom of the beaker. The Bi_2S_3 nanotubes were washed several times with ethanol, and then dispersed in a non-polar solvent such as cyclohexane.

Characterization. The powder X-ray diffraction (XRD) pattern was recorded with a Bruker D8 advance X-ray powder diffractometer with Cu Kα radiation (λ = 1.5406 Å), keeping the operating voltage and current at 40 kV and 40 mA, respectively. The 2θ range used was from 10 to 70° in steps of 0.02° with a count time of 2 s. The size and morphology of as-synthesized samples were determined by using a Hitachi model H-800 TEM (transmission electron microscopy). energy dispersive spectroscopy (EDX) was recorded to determine the composition of the products on a JEOL-2010F high-resolution TEM (HRTEM). Samples for TEM and HRTEM observation were prepared by placing a drop of a dilute cyclohexane dispersion of the nanocrystals on the surface of a copper grid.

2. Results and discussion

In our synthesis, $Bi(NO_3)_3{\cdot}5H_2O$ and S were mixed in a warm solvent, ODA. After stirring for a period of time, the system was heated to a higher temperature for further growth and crystallization. This simple process was carried out in an open beaker in air and degassing was not necessary. All the diffraction peaks in the powder XRD pattern of the product (Fig. 1) can be assigned to the orthorhombic phase Bi_2S_3 with lattice constants a = 11.15 Å, b = 11.304 Å, and c = 3.981 Å (JCPDS 17-0320). No characteristic peaks of any other phases are detected, indicating the high purity of the product.

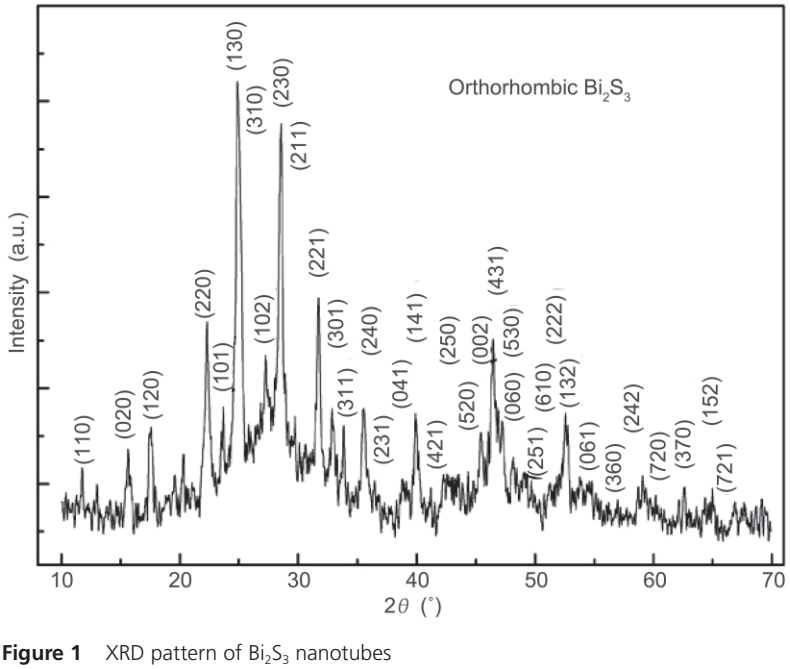

Figure 1 XRD pattern of Bi_2S_3 nanotubes

TEM and HRTEM were used to study the morphology and structure of the final product. Figure 2(a) shows the TEM image of Bi_2S_3 which exhibits tubular shape with lateral diameter of about 20 nm and length of about 160 nm. From the HRTEM image of an individual tube (Fig. 2(c)), the presence of groove-like structures can be clearly observed, further confirming the formation of Bi_2S_3 nanotubes with wall thickness of about 7 nm and central tubule diameter of about 6 nm. Figure 2(c) also shows clearly the multi-walled structure of a Bi_2S_3 nanotube which is composed of regularly ordered molecular layers and possesses a low density of defects such as stacking faults and missing layers. The measured spacings of the lattice planes revealed in the inset of Fig. 2(c) are about 0.399 and 0.196 nm, which are consistent with the separations of (220) planes and (002) planes of orthorhombic Bi_2S_3. The plane (002) is perpendicular to the axis of the nanotube, indicating that the nanotube grows along the [001] direction (*c*-axis). The HRTEM image (Fig. 2(d)) and the lattice fringes (Fig. 2(d), inset) of the tip of a single tube are consistent with the central section, indicating the uniform structure of the nanotube. They also reveal that the tube is open-ended. EDX was performed on a single nanotube to further determine its composition. From the spectrum in Fig. 2(b), we can see that only Bi and S peaks are observed together with the Cu peak which is generated by the copper grid. The atomic ratio of Bi and S (nearly 2 : 3) is consistent with the XRD result. This strategy for the synthesis of Bi_2S_3 nanotubes can be easily scaled up to provide gram-scale samples even in the laboratory. For example, when 2.5 g of $Bi(NO_3)_3{\cdot}5H_2O$ and 0.25 g of S were used as precursors, nearly 1 g of high quality product could be obtained successfully. Therefore, the as-developed solution-based method has the merits of yielding Bi_2S_3 nanotubes in a large amount and with high productivity, which is of great importance for future industrial applications of this material.

In order to understand the growth of the Bi_2S_3 nanotubes, we first need to study its crystal structure. As shown in Fig. 3(a), orthorhombic Bi_2S_3 has a highly anisotropic layered structure. It consists of infinite ribbon-like Bi_4S_6 polymers, which are linked together by intermolecular attraction between Bi and

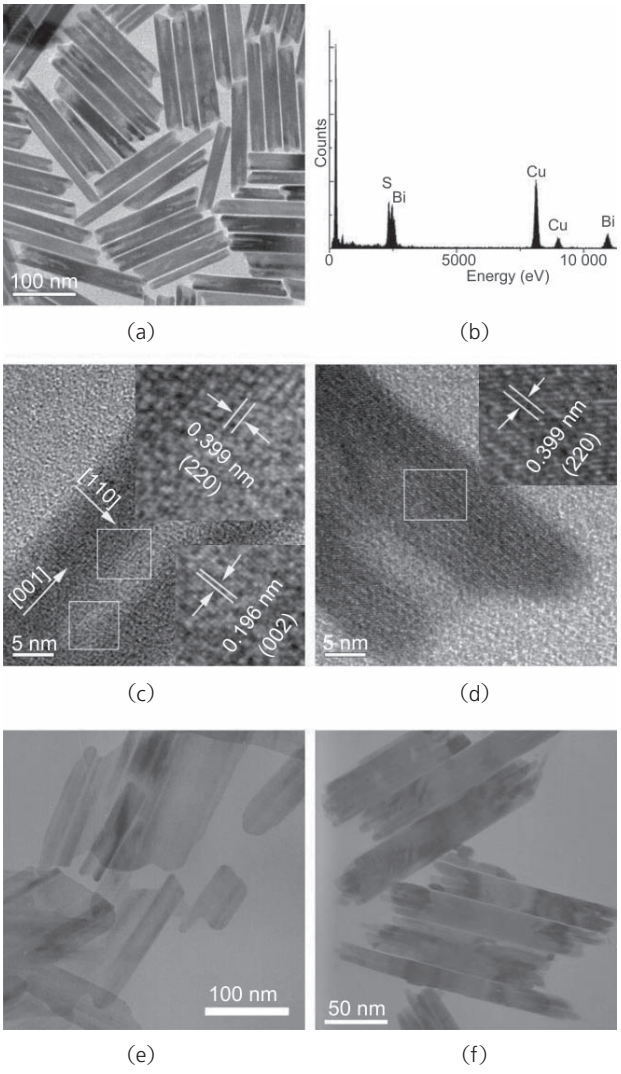

Figure 2 (a)TEM image of Bi_2S_3 nanotubes; (b) EDS analysis of a single Bi_2S_3 nanotube; (c) HRTEM image of a single tube; (d) HRTEM image of the tip of a single tube; (e) TEM image of Bi_2S_3 with sheet-like as well as a half-rolled structures; (f) TEM image of Bi_2S_3 with rod-bundle nanostructures

S atoms. The chain-like building blocks are parallel to the *c*-axis [23]. Therefore, Bi_2S_3 has a strong tendency toward 1-D growth along the [001] direction, which may lead to the formation of 1-D nanostructures such as nanorods, nanowires, nanoribbons, and nanotubes. In the present system, Bi_2S_3 nanotubes can form without the aid of shape-regulating catalysts or templates and they grow along the *c*-axis, indicating that the intrinsic nature of the material plays the most important role in directing the growth of Bi_2S_3 nanostructures. On the other hand, the preferential formation of nanotubes or other 1-D nanostructure depends on controlled experimental conditions. For

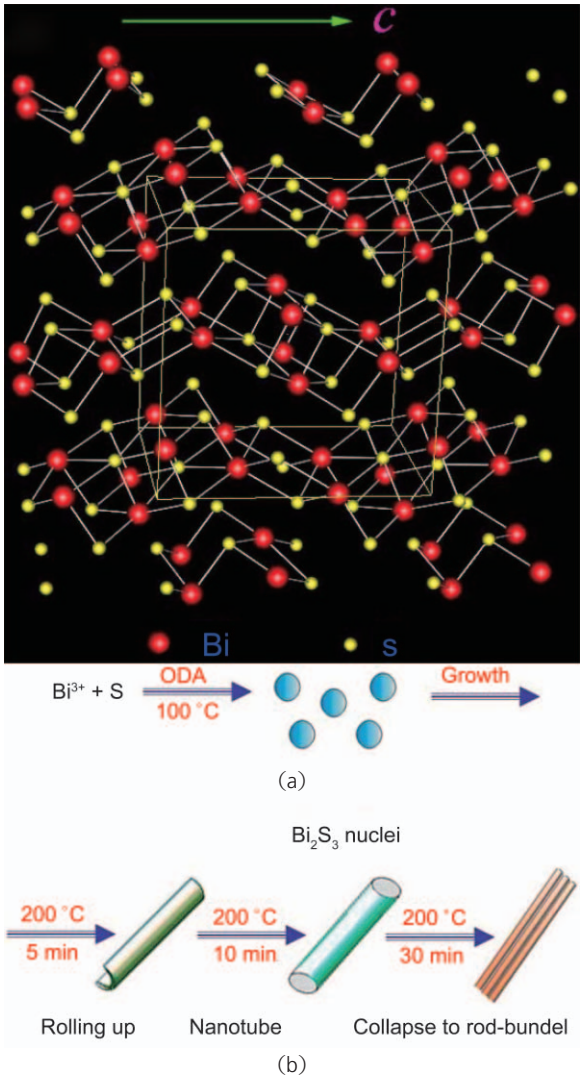

Figure 3 (a) Crystal structure of Bi_2S_3; (b) schematic depiction of the proposed growth mechanism for Bi_2S_3 nanotubes

the growth of inorganic nanotubes, there is a classic mechanism inspired by the natural phenomena of a piece of foliage or a piece of wet paper curling into scrolls during its drying process, namely, the rolling mechanism [24]. This concept was derived from the successful synthesis of nanotubes of carbon and other inorganic materials with layered structures in their bulk crystals such as Bi, BN, MoS_2, and WS_2 [2, 24–26]. When the interaction between neighboring layers is reduced at the edges of the layer, nanotubes will form through the rolling of these lamellar structures. In our synthesis, the growth of a Bi_2S_3 nanotube involves two stages: the nucleation process at low temperature and the subsequent growth step at higher temperature, as illustrated in Fig. 3(b). When white $Bi(NO_3)_3{\cdot}5H_2O$ and yellow S were added to ODA at 100 °C, the color of the solution changed to black, which was an indication of the formation of Bi_2S_3 nuclei. No crystalline products could be obtained at this stage and higher temperature was needed for their further growth and crystallization. When the system was heated to 200 °C, the nuclei self-assembled into lamellar structures driven by the anisotropic growth tendency of Bi_2S_3. The lamellar intermediates subsequently rolled up from the edges because sufficient energy was provided to overcome the strain energy barrier. After 10 min, the rolling process was complete and uniform Bi_2S_3 nanotubes were obtained. If the heating time was prolonged, the tubes broke down to afford rod-bundles. As direct experimental evidence to support above proposed growth process of Bi_2S_3, sheet-like as well as half-rolled structures co-existed when the reaction time was only 5 min (Fig. 2(e)), when the reaction time was 30 min, Bi_2S_3 with rod-bundle nanostructures could be observed (Fig. 2(f)).

3. Conclusions

In summary, we have designed a facile and economical approach to fabricate uniform Bi_2S_3 nanotubes. This method can provide gram-scale products even in the laboratory and can easily be expanded to the industrial scale, which is very important as far as applications of the material are concerned. The growth process was investigated and the classic rolling mechanism was proposed to be responsible for the nanotube formation.

Acknowledgements

This work is supported by National Science Foundation of China (NSFC) (90606006), the State Key Project of Fundamental Research for Nanoscience and Nanotechnology (2006CB932300), the Key Grant Project of Chinese Ministry of Education (No. 306020) and the National Undergraduate Innovation Training Project.

References

[1] Iijima, S. Helical microtubules of graphitic carbon. *Nature*

1991, *354*, 56–58.

[2] Tenne, R.; Margulis, L.; Genut, M.; Hodes, G. Polyhedral and cylindrical structures of tungsten disulphide. *Nature* **1992**, *360*, 444–446.

[3] Fan, S. S.; Chapline, M. G.; Franklin, N. R.; Tombler, T. W.; Cassell, A. M.; Dai, H. J. Self-oriented regular arrays of carbon nanotubes and their field emission properties. *Science* **1999**, *283*, 512–514.

[4] Huang, Y.; Duan, X. F.; Wei, Q. Q.; Lieber, C. M. Directed assembly of one-dimensional nanostructures into functional networks. *Science* **2001**, *291*, 630–633.

[5] Xia, Y. N.; Yang, P. D.; Sun, Y. G.; Wu, Y. Y.; Mayers, B.; Gates, B.; Yin, Y. D.; Kim, F.; Yan, Y. Q. One-dimensional nanostructures: Synthesis, characterization, and applications. *Adv. Mater.* **2003**, *15*, 353–389.

[6] Peng, H. L.; Xie, C.; Schoen, D. T.; Mcllwrath, K.; Zhang, X. F.; Cui, Y. Ordered vacancy compounds and nanotube formation in $CuInSe_2$–CdS core-shell nanowires. *Nano Lett.* **2007**, *7*, 3734–3738.

[7] Wang, M. S.; Kaplan-Ashirl, I.; Wei, X. L.; Rosentsveig, R.; Wagner, H. D.; Tenne, R.; Peng, L. M. *In situ* TEM measurements of the mechanical properties and behavior of WS_2 nanotubes. *Nano Res.* **2008**, *1*, 22–31.

[8] Cao, Q.; Rogers, J. A. Random networks and aligned arrays of single-walled carbon nanotubes for electronic device applications. *Nano Res.* **2008**, *1*, 259–272.

[9] Matsumoto, T.; Komatsu, T.; Arai, K.; Yamazaki, T.; Kijima, M.; Shimizu, H.; Takasawa, Y.; Nakamura, J. Reduction of Pt usage in fuel cell electrocatalysts with carbon nanotube electrodes. *Chem. Commun.* **2004**, 840–841.

[10] Cheng, F. Y.; Chen, J. Storage of hydrogen and lithium in inorganic nanotubes and nanowires. *J. Mater. Res.* **2006**, *21*, 2744–2757.

[11] Shimoda, H.; Gao, B.; Tang, X. P.; Kleinhammes, A.; Fleming, L.; Wu, Y.; Zhou, O. Lithium intercalation into opened single-wall carbon nanotubes: Storage capacity and electronic properties. *Phys. Rev. Lett.* **2002**, *88*, 015502.

[12] Dominko, R.; Arcon, D.; Mrzel, A.; Zorko, A.; Cevc, P.; Venturini, P.; Gaberscek, M.; Remskar, M.; Mihailovic, D. Dichalcogenide nanotube electrodes for Li-ion batteries. *Adv. Mater.* **2002**, *14*, 1531–1534;

[13] Wang, G. X.; Bewlay, S.; Yao, J.; Liu, H. K.; Dou, S. X. Tungsten disulfide nanotubes for lithium storage. *Electrochem. Solid-State Lett.* **2004**, *7*, A321–A323.

[14] Miller, B.; Heller, A. Semiconductor liquid junction solar cells based on anodic sulphide films. *Nature* **1976**, *262*, 680–681.

[15] Rabin, O.; Perez, J. M.; Grimm, J.; Wojtkiewicz, G.; Weissleder, R. An X-ray computed tomography imaging agent based on long-circulating bismuth sulphide nanoparticles. *Nat. Mater.* **2006**, *5*, 118–122.

[16] Zhang, B.; Ye, X. C.; Hou, W. Y.; Zhao, Y.; Xie, Y. Biomolecule-assisted synthesis and electrochemical hydrogen storage of Bi_2S_3 flowerlike patterns with well-aligned nanorods. *J. Phys. Chem. B* **2006**, *110*, 8978–8985;

[17] Li, L. S.; Sun, N. J.; Huang, Y. Y.; Qin, Y.; Zhao, N. N.; Gao, J. N.; Li, M. X.; Zhou, H. H.; Qi, L. M. Topotactic transformation of single-crystalline precursor discs into disc-like Bi_2S_3 nanorod networks. *Adv. Funct. Mater.* **2008**, *18*, 1194–1201.

[18] Ye, C. H.; Meng, G. W.; Jiang, Z.; Wang, Y. H.; Wang, G. Z.; Zhang, L. D. Rational growth of Bi_2S_3 nanotubes from quasi-two-dimensional precursors. *J. Am. Chem. Soc.* **2002**, *124*, 15180–15181.

[19] Ota, J. R.; Srivastava, S. K. Low temperature micelle-template assisted growth of Bi_2S_3 nanotubes. *Nanotechnology* **2005**, *16*, 2415–2419.

[20] Shen, X. P.; Yin, G.; Zhang, W. L.; Xu, Z. Synthesis and characterization of Bi_2S_3 faceted nanotube bundles. *Solid State Commun.* **2006**, *140*, 116–119.

[21] Jiang, J.; Yu, S. H.; Yao, W. T.; Ge, H.; Zhang, G. Z. Morphogenesis and crystallization of Bi_2S_3 nanostructures by an ionic liquid-assisted templating route: Synthesis, formation mechanism, and properties. *Chem. Mater.* **2005**, *17*, 6094–6100.

[22] Tang, J.; Alivisatos, A. P. Crystal splitting in the growth of Bi_2S_3. *Nano Lett.* **2006**, *6*, 2701–2706.

[23] Comor, M. I.; Dramicanin, M. D.; Rakocevic, Z.; Zec, S.; Nedeljkovic, J. M. Preparation of Bi_2S_3 quantum dots by dissolution of crystalline powder in acetonitrile. *J. Mater. Sci. Lett.* **1998**, *17*, 1401–1402.

[24] Li, Y. D.; Wang, J. W.; Deng, Z. X.; Wu, Y. Y.; Sun, X. M.; Yu, D. P.; Yang, P. D. Bismuth nanotubes: A rational low-temperature synthetic route. *J. Am. Chem. Soc.* **2001**, *123*, 9904–9905.

[25] Feldman, Y.; Wasserman, E.; Srolovitz, D. J.; Tenne, R. High-rate, gas-phase growth of MoS_2 nested inorganic fullerenes and nanotubes. *Science* **1995**, *267*, 222–225.

[26] Chopra, N. G.; Luyken, R. J.; Cherrey, K.; Crespi, V. H.; Cohen, M. L.; Louie, S. G.; Zettl, A. Boron nitride nanotubes. *Science* **1995**, *269*, 966–967.